

## EMG BASED CONTROL OF WRIST EXOSKELETON

MOHD SAFIRIN KARIS<sup>1\*</sup>, HYREIL ANUAR KASDIRIN<sup>2</sup>, NORAFIZAH ABAS<sup>2</sup>,  
WIRA HIDAYAT MOHD SAAD<sup>3</sup> AND MOHD SHAHRIEEL MOHD ARAS<sup>2</sup>

<sup>1</sup>*Faculty of Electrical and Electronic Engineering Technology,  
Universiti Teknikal Malaysia Melaka,  
75450 Ayer Keroh, Melaka, Malaysia*

<sup>2</sup>*Faculty of Electrical Engineering, Universiti Teknikal Malaysia Melaka,  
76100 Durian Tunggal, Melaka, Malaysia, Malaysia*

<sup>3</sup>*Faculty of Electronic and Computer Engineering, Universiti Teknikal Malaysia Melaka,  
76100 Durian Tunggal, Melaka, Malaysia, Malaysia*

\*Corresponding author: [safirin@utem.edu.my](mailto:safirin@utem.edu.my)

(Received: 23 March 2023; Accepted: 27 May 2023; Published on-line: 4 July 2023)

**ABSTRACT:** The significance of human motion intentions in a designed exoskeleton wrist control hand is essential for stroke survivors, thus making EMG signals an integral part of the overall system is critically important. However, EMG is a nonlinear signal that is easily influenced by several errors from its surroundings and certain of its applications require close monitoring to provide decent outcomes. Hence, this paper proposes to establish the relationship between EMG signals and wrist joint angle to estimate the desired wrist velocity. Fuzzy logic has been selected to form a dynamic modelling of wrist movement for a single muscle at different MVC levels and double muscles at a similar MVC level. The physical model of the exoskeleton hand using Simmechanics Matlab software has been developed to validate the performance of the fuzzy logic output result from both dynamic modelling approaches. A PID controller has been developed to smooth the exoskeleton hand movement fluctuations caused by the fuzzy logic decision-making process. As a conclusion, results showed a strong relationship between EMG signals and wrist joint angle improved the estimation results of desired wrist velocity for both dynamic modelling approaches hence strengthened the prediction process by providing a myoelectronic control device for the exoskeleton hand.

**ABSTRAK:** Kepentingan dalam mengetahui kehendak gerakan pergelangan tangan manusia adalah penting untuk pesakit strok yang terselamat, justeru menjadikan isyarat EMG amat penting pada keseluruhan sistem. Walau bagaimanapun, EMG adalah isyarat tidak linear yang mudah dipengaruhi ralat sekitaran dan memerlukan pemantauan rapi bagi hasil yang baik. Oleh itu, kajian ini mencadangkan kewujudan hubungan antara isyarat EMG dan sudut sendi pergelangan tangan bagi menganggarkan halaju pergelangan tangan yang dikehendaki. Logik kabur (*fuzzy logic*) telah dipilih bagi membentuk model dinamik pergerakan pergelangan tangan pada otot tunggal di tahap MVC yang berbeza dan otot berganda pada tahap MVC yang serupa. Model fizikal rangka luar tangan menggunakan perisian Matlab Simmekanik telah dibangunkan bagi mengesahkan prestasi Logik Kabur daripada kedua-dua pendekatan model dinamik. Pengawal PID telah dibangunkan bagi melicinkan gerakan turun naik tangan yang disebabkan proses membuat keputusan oleh Logik Kabur. Sebagai kesimpulan, dapatan kajian menunjukkan hubungan yang kukuh antara isyarat EMG dan sudut sendi pergelangan tangan. Ini meningkatkan anggaran dapatan halaju pergelangan tangan yang dikehendaki bagi kedua-dua pendekatan model dinamik seterusnya mengukuhkan proses ramalan melalui peranti kawalan mioelektronik rangka tangan.

**KEYWORDS:** *myoelectronic; fuzzy logic; PID controller; exoskeleton wrist design*

## 1. INTRODUCTION

Good health is a vital component for humans to emphasise life's quality by giving a person the best potential to face all of life's problems. This element might be degraded due to so many factors and one of them is stroke. In 2019, stroke overtook heart disease and pneumonia to become the third-leading cause of mortality globally and the second-leading cause of disability in Malaysia [1]. The most prevalent causes include hypertension (high blood pressure), diabetes, high cholesterol, irregular heartbeats, smoking, excessive alcohol use, inactivity, obesity, stress, and family history [1]. 75% of stroke survivors experience upper limb weakness, which includes constrained hand and wrist movement [2]. Based on this issue, stroke can disrupt a person's lifestyle, especially if it results in slow hand response, which restricts hand movement.

Degradation of hand function, which can be caused by stroke attack, may distract a brain signal from channelling user motion intention to control the hand movement. In general, hand structure is highly articulated, built up with many muscles' composition and bony segments. The main components of the hand are referred to in human anatomy as the palm, fingers, and wrist. There are various classifications of wrist movement, including neutral, flexion, extension, adduction, abduction, pronation, and supination [3]. These movements are directed by the user's motion intention which ultimately causes the user's hand muscles to contract, causing the user's hands to move [4]. This muscle excitation causes the Electromyography (EMG) signal to get excited. The EMG signal is a measure of electrical activity that spreads throughout the muscles and activates them. However, the desired wrist velocity and wrist joint angle position are correlated with this EMG signal strength [5].

To analyse the relationship between EMG signals, wrist joint angle position and desired wrist velocity, a physical model of the exoskeleton hand has been built up to mimic the human hand's articulated movement. The EMG signals collected from forearm muscles has served as the exoskeleton hand's primary input, and the wrist joint's placement angle has been increasing the accuracy of predictions of the desired wrist velocity. Given the significance of this relationship, it is important to include all of these factors as part of the control input so that the hand can move predictably whenever the muscles are flexed.

This written paper aims to analyse the relationship between EMG signals, wrist joint angle positioning, and desired wrist velocity. The output from this relationship has been expected to improve the output results for single muscles at different MVC levels and double muscles at similar MVC levels in wrist dynamic modelling approaches. After the decision-making process has been made, it has been tested on a virtual exoskeleton hand focusing on the desired wrist velocity.

## 2. MECHANICAL HAND DESIGN

The exoskeleton hand is designed to closely emulate the actual human hand that comprises of 5 fingers, a palm and a wrist that is attached to the forearm. The fingers comprise of 4 medial fingers with 3 bony segments and 1 thumb that has 2 bony segments. Based on hand anatomy, several hand measurements from ten male Asian subjects' aged from 21 to 40 years old following the anthropometric hand measurement have been collected. The mean of each measurement is illustrated in Table 1 below.

Table 1: Terminology on hand measurement

No	Finger	Hand Part	Mean [cm]
1	<b>Thumb</b>	Distal Phalanges Length	31.41
2		Proximal Phalanges Length	25.59
3		Distal Phalanges Breadth	18.26
4		Proximal Phalanges Breadth	16.67
5	<b>Index</b>	Distal Phalanges Length	23.94
6		Intermediate Phalanges Length	25.06
7		Proximal Phalanges Length	26.16
8		Distal Phalanges Length	14.55
9		Intermediate Phalanges Breadth	14.35
10		Proximal Phalanges Breadth	14.27
11	<b>Middle</b>	Distal Phalanges Length	25.15
12		Intermediate Phalanges Length	26.78
13		Proximal Phalanges Length	26.90
14		Distal Phalanges Breadth	14.01
15		Intermediate Phalanges Breadth	16.79
16		Proximal Phalanges Breadth	16.79
17	<b>Ring</b>	Distal Phalanges Length	24.36
18		Intermediate Phalanges Length	25.68
19		Proximal Phalanges Length	24.20
20		Distal Phalanges Length	13.62
21		Intermediate Phalanges Breadth	14.69
22		Proximal Phalanges Breadth	15.58
23	<b>Little</b>	Distal Phalanges Length	22.46
24		Intermediate Phalanges Length	15.28
25		Proximal Phalanges Length	15.89
26		Distal Phalanges Breadth	12.22
27		Intermediate Phalanges Breadth	13.26
28		Proximal Phalanges Breadth	14.54
29	<b>Palm</b>	Centre of Wrist crease to Middle	100.36
30		Centre of metacarpal	81.10
31		Hand Depth	47.60

The exoskeleton hand has been designed using measurements based on the collected anthropometry data. The design process began with the creation of each component, followed by their assembly into a single model or prototype as shown in Fig. 1. The exoskeleton hand design has been able to mimic natural human hand movement.

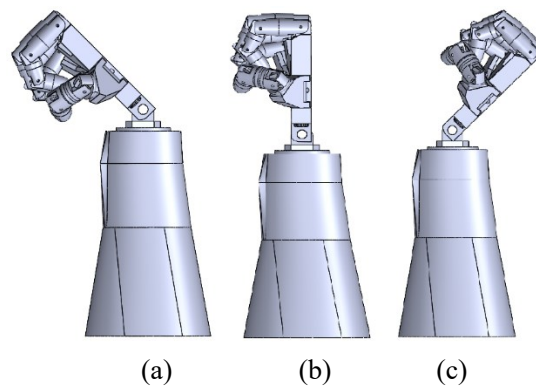


Fig. 1: Solidwork 3D Hand Design (a) Flexion Position, (b) Neutral Position, (c) Extension Position.

In this exoskeleton hand design, one degree of freedom (DoF) of wrist joint angle position has been focused on. This wrist movement covered three wrist hand joint angle positions namely, neutral ( $0^\circ$ ), flexion ( $-45^\circ$ ) and extension ( $45^\circ$ ). The exoskeleton hand has been designed under the fully actuated category since the exoskeleton hand wrist design can be moved towards achieving the desired wrist velocity. The flexibility of the hand has been designed to provide practical, typical hand movements.

### 3. EMG DATA COLLECTION

The samples came from male participants between the ages of 21 and 40. No neurological illnesses were present in any of the individuals, who were all in good health. The dominant hand has been chosen to collect the muscle movement-related EMG data. The palpate Scaphoid technique has been utilised to determine the wrist movement, and the medial epicondyle has been used to pinpoint the muscles' location [6]. For each position of wrist joint angle movement, a particular muscle has been activated in response to it. In this paper, the EMG signal values of the Flexor Carpi Radialis (FCR) and Extensor Carpi Radialis Longus (ECRL) has been used to represent each wrist joint angle movement [7].

Ten male subjects agreed to do the hand grip pattern experiment at different wrist joint angle positions by signing the consent form provided by the researcher. The experiment started as all the subjects were given detailed explanation of the procedure involved. Each experiment repeated three times [8]. The equipment used in this experiment, such as a hand dynamometer, LabQuest Mini data acquisitions by Vernier, EMG sensors by Vernier, a personal computer with Logger Lite data-collection software, a stopwatch, a protector and Kendall5400 diagnostic tab electrodes. All the experimental procedures were subject to the approval of the appropriate University Ethical Committee or Centre for Research and Innovation Management (CRIM) University Technical Malaysia Melaka (UTeM) Malaysia.

For the experimental procedures, subjects were instructed to use full hand grip strength to hold the hand dynamometer for five seconds, as shown in Fig. 2. The subject's greatest voluntary contraction was measured as the hand grip's maximal force (MVC). FCR and ECRL's muscles had electrode patches applied to the top of their abdominal muscles. The subjects were told to hold the hand dynamometer for five seconds while various hand grip strengths (20, 40, 60, 80, and 100% MVC) were utilised [8]. Rest periods were integrated for around two seconds after each grip. The Logger Lite software was used to record the extracted raw EMG signals. Then subjects repeated the same step as at  $0^\circ$  of wrist joint angle for different wrist positions (at  $45^\circ$  and  $-45^\circ$ ), as shown in Fig. 3 [9]. Figure 4 shows the EMG signals for the muscle excitation data parameters at different wrist joint angle hand positions.

### 4. EMG SIGNAL PROCESSING

The data that was collected was processed through several steps including detrend, filtering, feature extraction, and regression method. In the detrending process, data that did not begin at zero was moved to zero before proceeding to the following procedure. This approach improved amplitude readings by eliminating the inaccuracy caused by DC offset during the experimental procedure [10].

The feature of pre-processing EMG signals was extracted using a time domain method called Waveform Length (WL). In this study, WL technique has been used to extract the time-domain-based feature and measure the complexity of EMG signal excitation [11]. WL

is also defined as the cumulative length of waveform over the segment. Equation (1) below showed the equation modelled for the WL method.

$$WL = \sum_{i=1}^{N-1} |x_{i+1} - x_i| \quad (1)$$

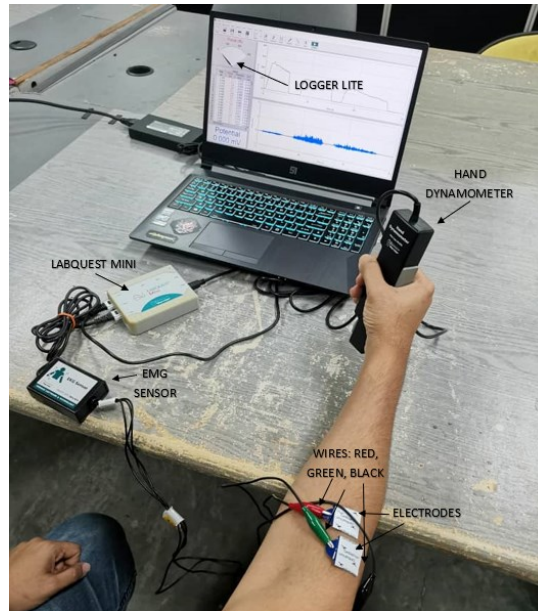


Fig. 2: Experimental set-up.

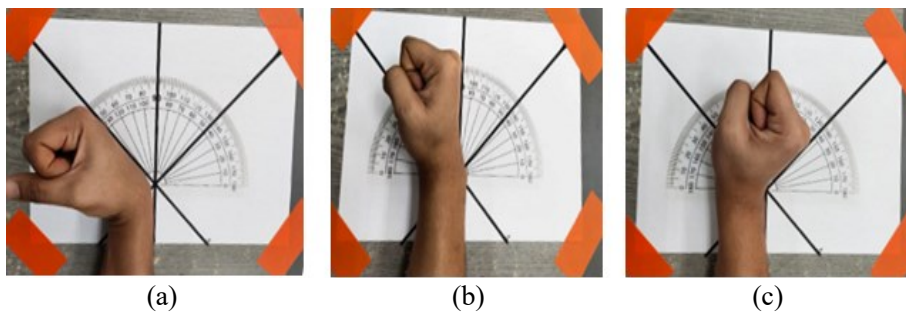


Fig. 3: Hand grasping positions for various wrist angle positions:  
 (a) at  $-45^\circ$ , (b) at  $0^\circ$ , and (c) at  $45^\circ$ .

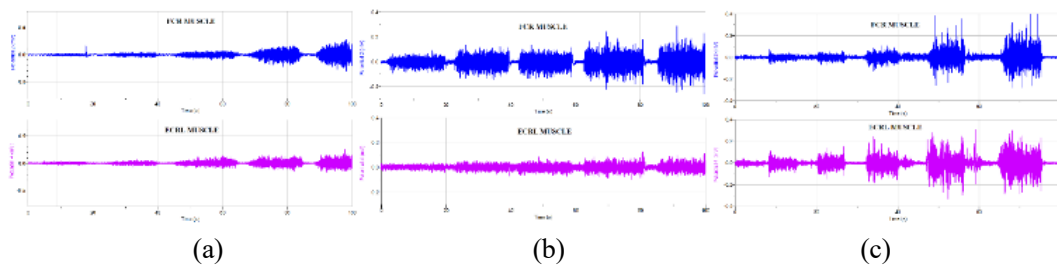


Fig. 4: EMG muscle excitations at different wrist joint angle positions,  
 (a) neutral, (b) flexion, (c) extension.

The sampling frequency was selected to be 1 kHz (i.e.,  $T=1$  ms) [8] as the acceptable sampling time ranges between frequencies of 200 and 2000 Hz. The recorded EMG voltages

were successfully processed within a 128 ms (sliding) time span and the analysis window increment was set to 50%, which is the interval between two adjacent windows.

The EMG signal was filtered using a second-order band-pass Butterworth filter with a cut-off frequency of 2 Hz (10-350Hz) [12]. A Butterworth filter rejects particular frequencies while allowing signals between two designated frequencies to flow through. Because the EMG signal ranged from 2-45Hz, 10-350Hz filters were applied.

To standardise EMG measurements, the maximum voluntary contraction (MVC) recorded individually from each subject was employed. This mechanism regulated the scaled value between 0 and 1 based on the measurement [13]. The data for each joint angle was normalised by subtracting the smallest joint angle for each sample and dividing it by its mean value. MVC-normalizing is one of the most extensively used normalisation algorithms [14].

## 5. DYNAMIC MODELLING OF WRIST MOVEMENT USING FUZZY LOGIC

Input signals derived from EMG signals, wrist joint angle position, and desired wrist velocity were predicted to be related. Dynamic modelling was utilised to model the relationship between these three parameters to analyse this relationship. According to the experimental results, EMG signals generated by muscle excitement are directly proportional to wrist joint angle position. As a result, the appropriate wrist desired velocity was determined by this relationship. Fuzzy logic was utilised to perform the prediction mapping between these three parameters.

### 5.1 Dynamic Modelling on Single Muscle at Different MVC Level

The FL's three inputs recorded EMG signals from the forearm muscles and wrist joint angle position. The desired velocity of the hand wrist was chosen as the FL's output since it has one of the most common control theories for exoskeleton hand systems [4]. The activation rate of the extensor and flexor muscles was continuously assessed utilising EMG signal data and WL feature extraction algorithms.

The FLC's structure consists of fuzzification, a rule table, a fuzzy inference system, and a defuzzification algorithm [7]. As seen in Fig. 5, fuzzy logic first fuzzifies the input variables before building the rule table with membership functions. A Mamdani-type fuzzy inference system was used to map the inputs to the output by merging all of the linguistic claims in the rule table. Finally, the defuzzification operation was carried out using a "centroid" technique that returns the area centre beneath the curve [7]. FCR and ECRL muscle values were analysed separately in this design based on their performance at different MVC (20%, 60%, and 100%) with various wrist joint angle positions to predict the wrist desired velocity.

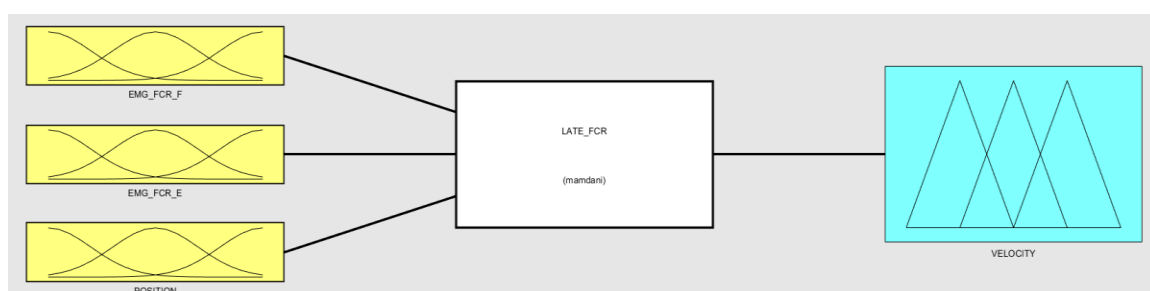


Fig. 5: Fuzzy logic single muscle design.

As the first stage in the fuzzy logic process, the input variables have been fuzzified using membership functions that can take several forms. Figure 6(a), 6(b), and 6(c) below showed three triangular-shaped membership functions that have been used to fuzzify EMG signals and two trapezoidal-shaped membership functions that have been used to fuzzify wrist joint angle position. The input to the FCR and ECRL muscles has been analysed in two stages: EMG\_F (EMG value while the wrist was in flexion position) and EMG\_E (EMG value while the wrist was in extension position). EMG signals are classified as SMALL (S), MEDIUM (M), and HIGH (H). Input triangular membership functions are defined based on the testing data after passing through the feature extraction process. For input, the highest and lowest data numbers were taken from their own group dataset to form this triangular membership function.

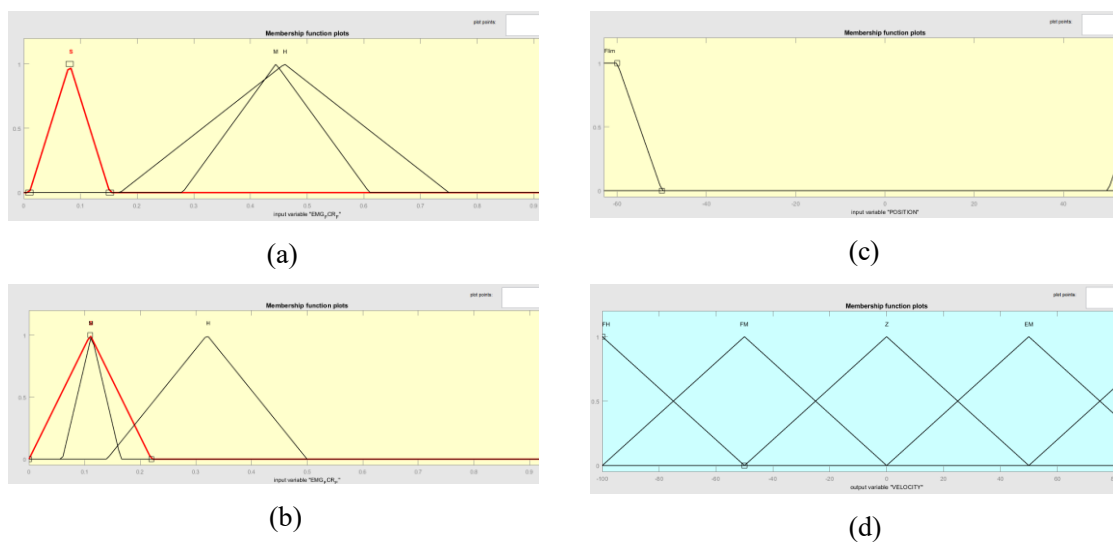


Fig. 6: (a) Function of triangular-shaped membership used for EMG signal (EMG\_F), (b) Function of triangular-shaped membership used for EMG signal (EMG\_E), (c) Function of trapezoidal-shaped membership used for wrist joint angle (POSITION), (d) Function for triangular membership used for the desired wrist velocity.

The output desired wrist velocity of fuzzy logic used five triangular-shaped membership functions. The performance of the fuzzy technique, which was chosen as the wrist desired velocity, was categorized as FH (flexion high: 100°/s), FM (flexion medium: 50°/s), Z (zero velocity: 0°/s), EM (extension medium: 50°/s) and EH (extension high: 100°/s) as illustrated in Fig. 6(d).

Table 2 shows the rule table for 15 IF-THEN rule statements. EMG\_F and EMG\_E are signals generated during the wrist joint angle for flexion and extension. The EMG signals produced by both flexion and extension actions should yield zero wrist velocity, as shown in the first three basic criteria in Table 2. The next six rules examined the different EMG signal excitations to predict the wrist desired velocity. To round out the fifteen criteria, there were rules that limited the device's wrist joint angle as well as provided further safety measures for the desired wrist velocity.

The 15 linguistic statements in the rule table were all combined to form a Mamdani-style fuzzy inference method that maps the inputs to the output. The conjunction expression AND in these sentences corresponds to a minimal operator that selects only the lowest of the fuzzified inputs. For each IF-THEN rule statement, an implication operation was performed using the "minimum" method, which directly truncates the fuzzy output sets. Instead, at the

end, a complex-shaped curve was generated by aggregating all the trimmed fuzzy output sets using the "maximum" method.

Table 2: 15 IF-THEN rule statements [7].

No	EMG_F	EMG_E	Wrist Position	Wrist Velocity
1	if S	S	then	Z
2	if M	M	then	Z
3	if H	H	then	Z
4	if M and S	and not Elim	then	FM
5	if H and M	and not Elim	then	FM
6	if H and S	and not Elim	then	FH
7	if S and M	and not Elim	then	EM
8	if M and H	and not Elim	then	EM
9	if S and H	and not Elim	then	EH
10	if M and S	and Elim	then	Z
11	if H and M	and Elim	then	Z
12	if H and S	and Elim	then	Z
13	if S and M	and Elim	then	Z
14	if M and H	and Elim	then	Z
15	if S and H	and Elim	then	Z

### 5.1.1 Fuzzy Logic Output Design for Dynamic Modelling on Single Muscle at Different MVC Level

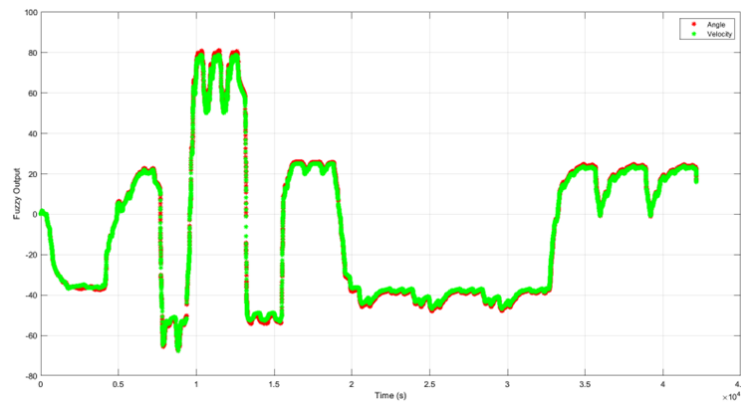


Fig. 7: FCR muscle response from fuzzy logic output.

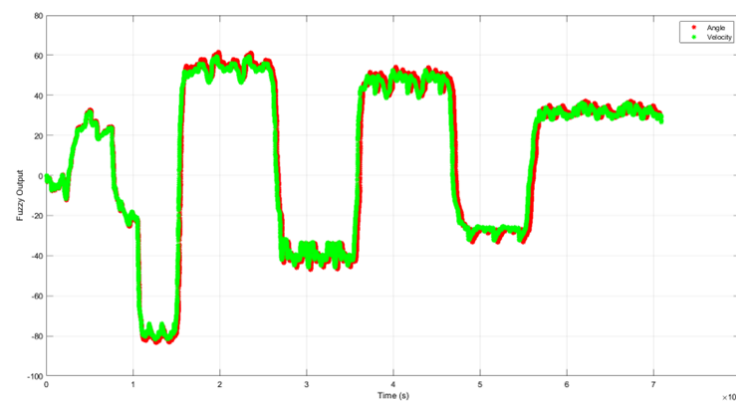


Fig. 8: ECRL muscle response from fuzzy logic output.

Figures 7 and 8 depict the output response of fuzzy logic depending on various MVC muscle levels and wrist joint angle movements. Based on these output results, identical levels of MVC should generate a velocity value of zero. As the Input signal from EMG\_F became greater than EMG\_E, the velocity of the hand shifted from extension to flexion and vice versa. When the tested data was compared to the bigger or lesser value than the other, it generated different amplitude values for the wrist's desired velocity.

## 5.2 Dynamic Modelling on Double Muscles at Similar MVC Level

The FL's two inputs recorded EMG signals from two forearm muscles. As one of the most popular control theories for exoskeleton hand systems, the desired velocity of the hand wrist was selected as the FL's output [4]. The activation rate for extensor and flexor muscles of the EMG signal were continuously assessed using the WL feature extraction algorithms.

The structure of the FLC comprises fuzzification, a rule table, a fuzzy inference system, and a defuzzification mechanism [7]. Fuzzy logic first fuzzifies the input variables before designing the rule table using membership functions, as depicted in Fig. 9. A fuzzy inference system of the Mamdani type is used to map inputs to outputs by merging all linguistic statements in the rule table. The defuzzification step was completed using a "centroid" technique that returned the area's centre beneath the curve [7]. In this architecture, FCR and ECRL muscle values were simultaneously analysed based on their performance at different MVC levels (20% and 60%) and wrist joint angle positions to estimate the wrist's desired velocity.

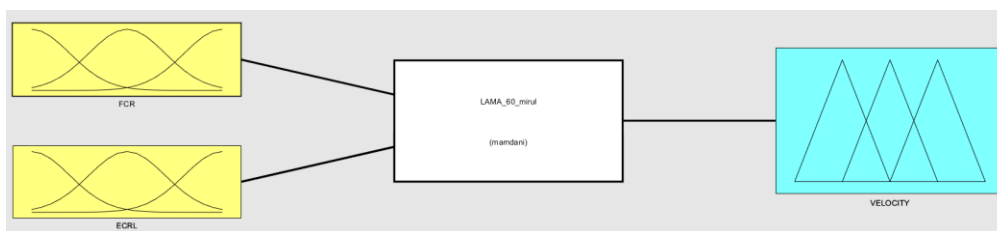


Fig. 9: Fuzzy logic double muscles design.

As the initial step of fuzzy logic, the input variables are first fuzzy - tuned using membership functions, which can take on a variety of shapes. As depicted in Fig. 10(a) and 10(b), three triangular-shaped membership functions are utilised to fuzzify EMG signals. Following the feature extraction procedure input triangular membership functions were defined based on the testing data. EMG signals were classified as SMALL (S), MEDIUM (M), and HIGH (H). To build this triangular membership function, the highest and lowest data numbers from their respective group dataset were used as input.

Five triangular-shaped membership functions were used to fuzzify desired wrist velocity fuzzy output depicted in Fig. 10(c). The performance of the desired wrist velocity was labelled as FH (flexion high: 100°/s), FM (flexion medium: 50°/s), Z (zero velocity: 0°/s), EM (extension medium: 50°/s) and EH (extension high: 100°/s).

Table 3 displays the rule table for 9 IF-THEN rule statements. During wrist flexion position, the FCR muscle gave most responsive signal level hence the parameter data was recorded, whereas the ECRL muscle signal level response was the most responsive during wrist extension position so the data being documented represented the extension state. The wrist velocity was suspected to produce zero state if the EMG signals generated by flexion and extension actions of wrist movement had similar value. The wrist velocity was determined by comparing the EMG signal level. If FCR value was greater than ECRL, FM was created, whereas if ECRL was greater than FCR, EM was produced. FH was formed

when the value of FCR was extremely bigger than ECRL, and EH was produced when the value of ECRL was extremely greater than FCR.

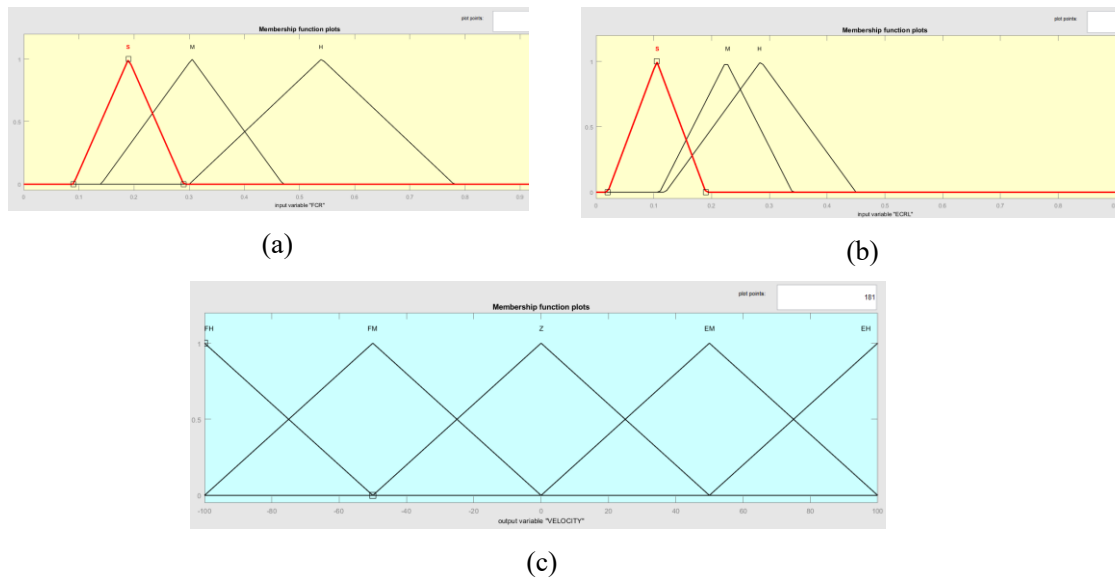


Fig. 10: (a) Function of triangular-shaped membership used for FCR Muscle, (b) Function of triangular-shaped membership used for ECRL Muscle, (c) Function for triangular membership used for the desired wrist velocity.

The 9 linguistic claims stated in rule Table 3 were synthesised into a Mamdani-style fuzzy inference system that mapped inputs to outputs. In these phrases, the conjunction AND represents a minimum operator that selects only the lowest of the fuzzy inputs. For each IF-THEN rule statement, an implication operation was performed using the "minimum" method, which directly truncated the fuzzy output sets. Instead, a complex-shaped curve was generated at the conclusion by aggregating all fuzzy output sets that have been trimmed using the "maximum" method.

The FCR muscle was more aggressively stimulated when the wrist was in the flexion position, but the ECRL responded more aggressively when the wrist was in the extension position. In other instances, despite being in the opposite position, both muscles still produced EMG output signal voltages, but the reading was lower than the others. In contrast, when the wrist was in a neutral position, both EMG signal muscles should produce identically stimulated voltages of signal strength from both muscles.

Table 3: 9 IF-THEN rule statements

No		FCR Muscle		ECRL Muscle		Wrist Velocity
1	if	S	and	S	then	Z
2	if	M	and	M	then	Z
3	if	H	and	H	then	Z
4	if	M	and	S	then	FM
5	if	H	and	M	then	FM
6	if	H	and	S	then	FH
7	if	S	and	M	then	EM
8	if	M	and	H	then	EM
9	if	S	and	H	then	EH

The FCR muscle was more aggressively stimulated when the wrist was in the flexion position, but the ECRL responded more aggressively when the wrist was in the extension position. In other instances, despite being in the opposite position, both muscles still produced EMG output signal voltages, but the reading was lower than the others. In contrast, when the wrist was in a neutral position, both EMG signal muscles should produce identically stimulated voltages of signal strength from both muscles.

### 5.2.1 Fuzzy Logic Output Design for Dynamic Modelling on Double Muscle at Similar MVC Level

Figures 11 and 12 show both fuzzy output results for wrist desired velocity. As illustrated by Fig. 11, at a signal level of 20% MVC, it can be estimated that the data division readings represented on each wrist joint angle position tended to overlap with each other, hence producing an unstable desired wrist velocity output result. Fig. 12 depicts a considerable desired wrist velocity fuzzy output result, as each component of the wrist position can be easily recognized at 60% MVC. This contributed when the EMG signal value excitation began to exhibit its considerable group uniqueness characteristic during the feature extraction process, thus making the fuzzy desired wrist velocity output data easier to comprehend. The fuzzy logic output for Fig. 7, 8, 11, 12 showed a certain range that was significantly comparable for wrist desired velocity and wrist joint angle data collected in the experiment.

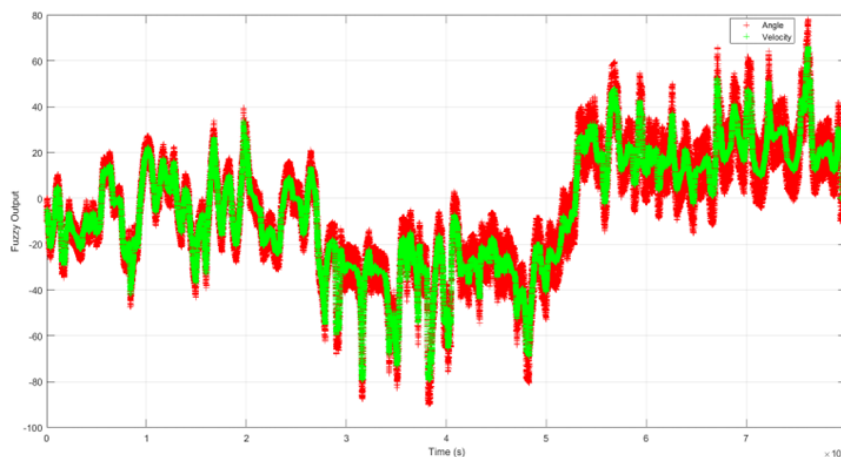


Fig. 11: Fuzzy output for 20% MVC.

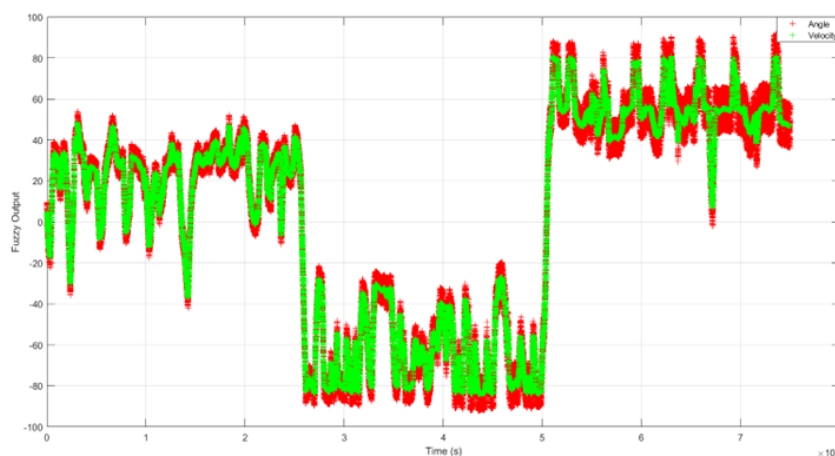


Fig. 12: Fuzzy output for 60% MVC.

## 6. PID CONTROL

PID controllers, which stands for proportional, integral, and derivative, employ a control loop feedback method to regulate process variables. The end-effector controller is configured according to Eq. (2):

$$f = J_a^T T_a = K_P e + K_D \dot{e} + K_I \int e dt \quad (2)$$

where  $K_P$ ,  $K_D$ ,  $K_I$  are some positive definite tuned parameter matrices. To compute the actuator torque  $T_a$ , use  $(J_a^T)^+$  to obtain as shown in Eq. (3):

$$T_a = (J_a^T)^+ (K_P e + K_D \dot{e} + K_I \int e dt) \quad (3)$$

The integral terms include eliminating or reducing the steady state error for tracking a step input signal. In actual implementation, the integral term is usually limited by some bounds. The main function of PID is to compensate for the fluctuation signal coming from the output mapping process, hence provide more stable continuous output control for the exoskeleton hand. In this paper, metaheuristic algorithm has been applied to obtain the value for  $K_P$ ,  $K_I$  and  $K_D$  [15]. The value for  $K_P = 3.97 \times 10^{-9}$ ,  $K_I = 0.11 \times 10^0$  and  $K_D = 1.44 \times 10^{-6}$ .

## 7. RESULTS AND DISCUSSIONS

### 7.1 Analysis of the Design Performance

The following step involves importing the SolidWorks file into MATLAB. At this point, any Simulink block, including Fuzzy Logic and PID, can be utilized to build a system to estimate the desired wrist velocity for the exoskeleton hand [16]. PID was utilised to control the output from the fuzzy logic to estimate the desired wrist velocity. For both fuzzy dynamic modelling approaches, identical plant was employed. The modifications were accomplished by modifying the input and fis files for fuzzy logic. Figure 13 depicts the completed development of the SimMechanics testing system for physical modelled of exoskeleton hands.

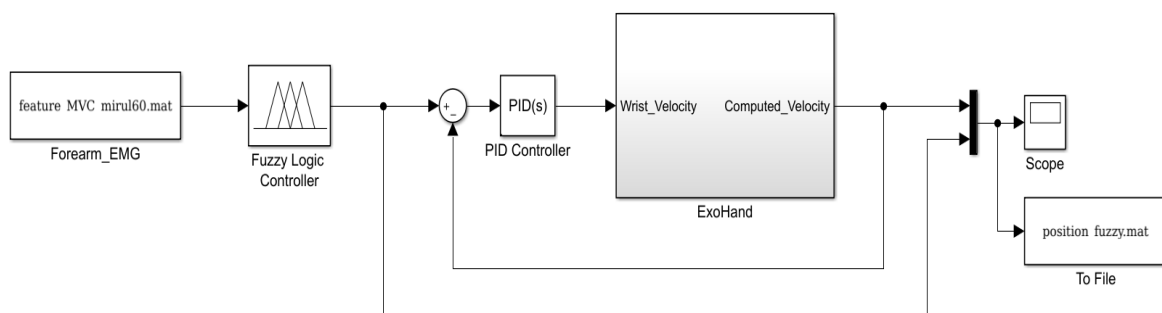


Fig. 13: Full system of exoskeleton hand for wrist movement with FL and PID controller.

### 7.2 Analysis of the Design Performance Using PID

#### 7.2.1 Analysis of Dynamic Modelling on Single Muscle at Different MVC Level

Figures 14 and 15 show the Fuzzy Logic and PID controller and fuzzy logic output result based on the performance of a single muscle affected on predicting wrist desired velocity of the exoskeleton hand system. Initially, fuzzy logic was used as the system's dynamic model. However, the output from the FL mapping process was fed to the exoskeleton hand modelled resulted in an unstable wrist velocity output result. The red line from both graphs originated from the FL decision making process. In Fig. 14, an obvious

case where an overshoot signal happened located between 200s to 400s while undershoot happened at 1400 s to 1600 s. In Fig. 15, a clear case of overshoot happened at 700s to 900s while undershoot case happened between 900 s to 1100 s. Due to this instability in the FL result, the PID controller was utilised to compensate for the fluctuation of the predicted output value. The blue line graph in each figure illustrates the exoskeleton hand output result after the PID controller was developed. The results were a more stable output for the exoskeleton hand, compensating for the fluctuations happening in the FL mapping process thus smoothing the movement at the desired exoskeleton hand wrist velocity.

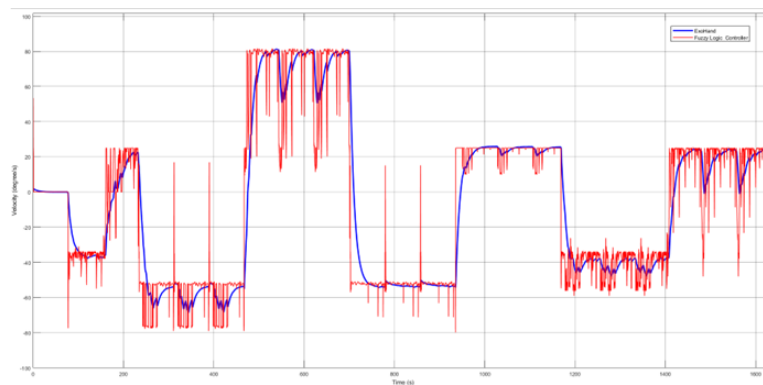


Fig. 14: Fuzzy Logic and PID controller for Estimated wrist desired velocity of Exoskeleton hand using FCR muscle.

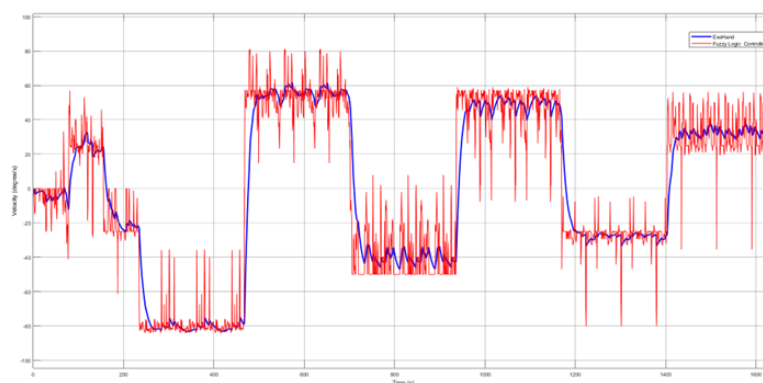


Fig. 15: Fuzzy Logic and PID controller for Estimated wrist desired velocity of Exoskeleton hand using ECRL muscle.

### 7.2.2 Analysis of Dynamic Modelling on Double Muscles at Similar MVC Level

Figures 16 and 17 show the desired wrist velocity output of the Fuzzy Logic and PID controller based on the performance of double muscles for the exoskeleton hand system. Fuzzy logic was chosen as the mapping technique for the exoskeleton hand system. This chosen method compared measurement data from each muscle's excitation group and used the results to predict the desired wrist velocity. Fig. 16 and 17 illustrate a red line graph representing a fluctuation of fuzzy output results. For both graphs, the pattern in each wrist desired velocity were related to EMG signal generation. In Fig. 16, the pattern generations were not too noticeable since the signal values were produced in closer range separation while in Fig. 17, the signal values produced were for larger range separation. To compensate for the fluctuations generated from Fuzzy logic's output, the PID was chosen as a controller. Through the use of the PID controller, the blue line graph in both Fig. 16 and 17 existed to smooth the fluctuation generated by the FL decision making process, hence producing

distinct wrist desired velocity output results at various wrist joint angle positions for the exoskeleton hand system.

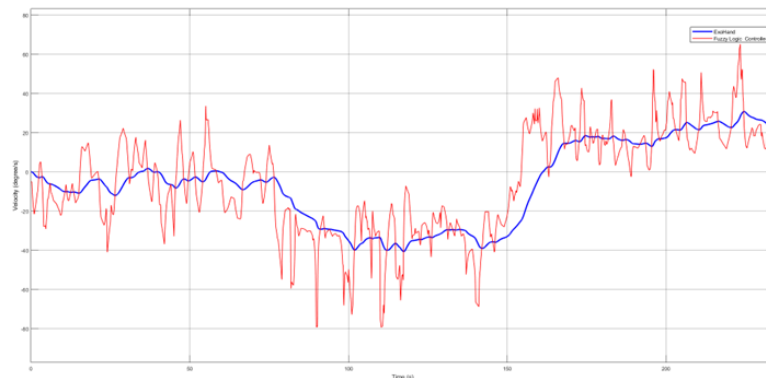


Fig. 16: Fuzzy Logic and PID controller for Estimated wrist desired velocity of Exoskeleton hand using FCR and ECRL muscles at 20% MVC.

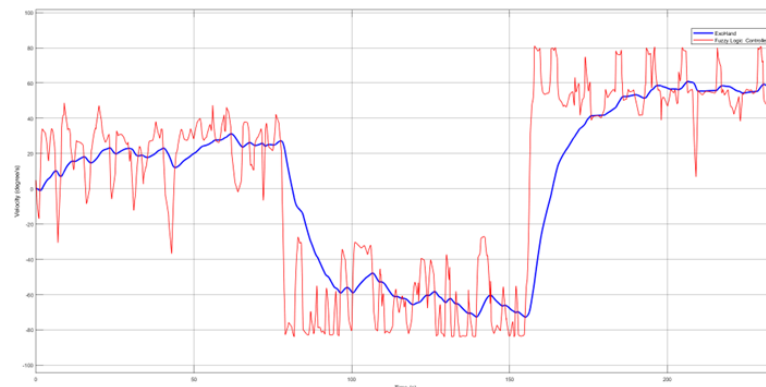


Fig. 17: Fuzzy Logic and PID controller for Estimated wrist desired velocity of Exoskeleton hand using FCR and ECRL muscles at 60% MVC.

## 8. CONCLUSION

Wrist hand position movement has become an integral component of human intentions in daily activities. Realizing the significance of this component, it is essential to emphasise the use of this wrist desired velocity estimation that follows the user's motion intention as employed in this paper, where it is also utilised for an exoskeleton hand and other rehabilitation applications. The relationship between and wrist joint angle hand position and EMG signal excitation can also be used to predict the assessment of the desired wrist velocity for the exoskeleton hand system.

Along the process to estimate the wrist desired velocity of the exoskeleton hand system, the feature extraction method needed to be selected properly. The collected data must pass through this process since it has been used to extract the usable data set to represent the EMG signals that are proportionally related to wrist joint angle position and desired wrist velocity of exoskeleton hand movement. Based on the calculation of standard deviation, Waveform length (WL) was chosen for the feature extraction method since it provides lower standard deviation value than Root Mean Square (RMS), Mean Absolute Value (MAV), Integrated EMG (IEMG), and Zero Crossing (ZC) [17]. By analysing these standard deviation values, the tabulation of data located in close proximity to one another produced more accurate estimates of the desired wrist velocity prior to the mapping stage [18].

The use of fuzzy logic as a dynamic modelling of the system gave the author an authority to design the exoskeleton hand system based on author logic control. However, the mapping process produced a fluctuation in estimating the desired wrist velocity output results. To compensate for the fluctuation generated, PID was chosen as a controller approach for this paper because of its simplicity and dependability in industrial applications. This controller has proven to reduce output volatility and stabilised desired wrist velocity output results. However, the exoskeleton hand's final results still contained some errors, as the hand's desired wrist velocity changed. An optimization method, such as Particle Swarm Optimization (PSO), Invasive Weed Optimization (IWO) or Firefly Algorithm (FA), could be utilised in future planning to adapt to nonlinear input derived from EMG data and wrist joint angle position and desired wrist velocity.

## ACKNOWLEDGMENT

The authors would like to thank the Ministry of Higher Education Malaysia for the financial support. The project is funded under Fundamental Research Grant Support. No (Ref: FRGS/1/2021/TK0/UTEM/02/54). The authors also want to thank Universiti Teknikal Malaysia Melaka for all the support.

## REFERENCES

- [1] McGowan B, "Industrial exoskeletons: what you're not hearing," *Occup. Heal. Saf. Mag.*, vol. 1, 2018.
- [2] Wahit MAA, Ahmad SA. (2018) Design and development of low-cost exoskeleton hand robot structure. *IEEE Student Conf. Res. Dev. Inspiring Technol. Humanit. SCOReD 2017 - Proc.*, vol. 2018-Jan, pp. 45-49. doi: 10.1109/SCOReD.2017.8305423.
- [3] Asogbon MG, Samuel OW, Jiang Y, Wang L, Geng Y, Sangaiah AK, Chen S, Fang P, and Li "Appropriate feature set and window parameters selection for efficient motion intent characterization towards intelligently smart emg-pr system," *Symmetry (Basel)*, vol. 12, no. 10, pp. 1–20, 2020, doi: 10.3390/sym12101710.
- [4] Zhang L, Qi W, Hu Y, and Chen Y, "Disturbance-observer-based fuzzy control for a robot manipulator using an EMG-driven neuromusculoskeletal model," *Complexity*, vol. 2020, 2020, doi: 10.1155/2020/8814460.
- [5] Chen C, Guo W, Ma C, Yang Y, Wang Z, and Lin C, "Semi-based continuous estimation of finger kinematics via large-scale temporal convolutional network," *Appl. Sci.*, vol. 11, no. 10, 2021, doi: 10.3390/app11104678.
- [6] Mendez V, Pollina L, Artoni F and Micera S, "Deep learning with convolutional neural network for proportional control of finger movements from surface EMG recordings," *Int. IEEE/EMBS Conf. Neural Eng. NER*, vol. 2021-May, pp. 1074–1078, 2021, doi: 10.1109/NER49283.2021.9441095.
- [7] Kilic E, Dogan E. (2017) Design and fuzzy logic control of an active wrist orthosis. *Proc. Inst. Mech. Eng. Part H J. Eng. Med.*, 231(8): 728-746. doi: 10.1177/0954411917705408.
- [8] Xu F, Zheng Y, and Hu X, "Estimation of joint kinematics and fingertip forces using motoneuron firing activities: A preliminary report," *Int. IEEE/EMBS Conf. Neural Eng. NER*, vol. 2021-May, pp. 1035–1038, 2021, doi: 10.1109/NER49283.2021.9441433.
- [9] Behrens M, Husmann F, Moeller AM, Schlegel J, Reuter EM, and Zschorlich VR, "Neuromuscular properties of the human wrist flexors as a function of the wrist joint angle," *Front. Bioeng. Biotechnol.*, vol. 7, no. AUG, 2019, doi: 10.3389/fbioe.2019.00181.
- [10] Kim S, Shin DY, Kim T, Lee S, Hyun JK, Park SM. (2022) Enhanced recognition of amputated wrist and hand movements by deep learning method using multimodal fusion of electromyography and electroencephalography. *Sensors*, 22(2): 1-17. doi: 10.3390/s22020680.

- 
- [11] Lara J, Paskaranandavadi N, and Cheng LK, “HD-EMG Electrode Count and Feature Selection Influence on Pattern-based Movement Classification Accuracy,” Proc. Annu. Int. Conf. IEEE Eng. Med. Biol. Soc. EMBS, vol. 2020-July, pp. 4787–4790, 2020, doi: 10.1109/EMBC44109.2020.9175210.
- [12] Hayashi H, Shibasaki T, and Tsuji T, “A Neural Network Based on the Johnson SU Translation System and Related Application to Electromyogram Classification,” IEEE Access, vol. 9, pp. 154304–154317, 2021, doi: 10.1109/ACCESS.2021.3126348.
- [13] Subasi A and Qaisar SM, “Surface EMG signal classification using TQWT, Bagging and Boosting for hand movement recognition,” J. Ambient Intell. Humaniz. Comput., vol. 13, no. 7, pp. 3539–3554, 2022, doi: 10.1007/s12652-020-01980-6.
- [14] Copaci D, Serrano D., Moreno L, and Blanco D, “A high-level control algorithm based on sEMG signalling for an elbow joint SMA exoskeleton,” Sensors (Switzerland), vol. 18, no. 8, 2018, doi: 10.3390/s18082522.
- [15] Joseph SB, Dada EG, Abidemi A, Oyewola DO, and Khammas BM, “Metaheuristic algorithms for PID controller parameters tuning: review, approaches and open problems,” Heliyon, vol. 8, no. 5, p. e09399, 2022, doi: 10.1016/j.heliyon.2022.e09399.
- [16] Tageldeen MK, Perumal N, Elamvazuthi I, and Ganesan T, “Design and control of an upper arm exoskeleton using Fuzzy logic techniques,” 2016 2nd IEEE Int. Symp. Robot. Manuf. Autom. ROMA 2016, pp. 1–6, 2017, doi: 10.1109/ROMA.2016.7847838.
- [17] Jia G, Lam HK, Liao J, Wang R. (2020) Classification of electromyographic hand gesture signals using machine learning techniques. Neurocomputing, 401: 236-248. doi: 10.1016/j.neucom.2020.03.009.
- [18] Bardizbanian B, Zhu Z, Li J, Huang X, Dai C, Luna CM, McDonald BE, Farrell TR, and Clancy EA, “Efficiently Training Two-DoF Hand-Wrist EMG-Force Models,” Proc. Annu. Int. Conf. IEEE Eng. Med. Biol. Soc. EMBS, vol. 2020-July, pp. 369–373, 2020, doi: 10.1109/EMBC44109.2020.9175675.